Changing Cellulose Crystalline Structure in Forming Wood Cell Walls

Yutaka Kataoka and Tetsuo Kondo*

Forestry and Forest Products Research Institute, P.O. Box 16, Tsukuba Norin, 305 Japan

Received February 8, 1996
Revised Manuscript Received July 18, 1996

Although the process of biosynthesis and subsequent crystallization of cellulose is the initial stage of plant cell wall formation, the *in vivo* mechanism for cellulose crystallization has still not been clearly resolved. Several years ago, Attala and VanderHart[1] found that the cellulose I crystalline structure is really a composite of two allomorphs, thereby providing a new method by which to investigate this mechanism. Why are two cellulose allomorphs, I_α and I_β, crystallized at the surface of plant cells? An earlier study[1] pointed out that cellulose from enlarging algae was rich in the I_α phase, whereas the I_β phase was the dominant cellulose component in higher plants which form thick secondary walls once the primary geometry of the cells has been established. More recently, following studies[2−5] have suggested that the metastable triclinic I_α phase is formed by some type of stress during crystallization, whereas the stable monoclinic I_β phase crystallizes in a relatively relaxed state. The nature or source of the stress, however, was not specified.

Here, we want to explore the idea that plant cellular forces exerted during growth have a direct influence on crystallization of newly biosynthesized cellulose which can be gel or a liquid crystal phase. This paper provides an *in vivo* evidence that the major crystalline component of cellulose changes from I_α to I_β when cellular enlarging growth ceases.

To examine the cellulose crystalline structure in a developing wood cell wall, we prepared 30-μm-thick radial (in the radial direction of the annual rings) sections of differentiating coniferous wood xylem obtained from *Cryptomeria japonica* (Japanese cedar) and *Chamaecyparis obtusa* (Japanese cypress).[6] In these sections, developing axial tracheids and their cell walls were lined up in order of maturity starting from the cambial zone (C) to the mature xylem (MX) as shown in Figure 1. The sections were disencrusted thoroughly[7] by a combination of two purification methods for primary wall[8] and for wood cell wall cellulose[9] and then were freeze-dried with *tert*-butyl alcohol.

The purified sections were analyzed with a FT-IR spectrometer (Nicolet Magna 550) equipped with a microscopic attachment (Nicolet Nic plan).[10] Spectra were obtained on small areas ($300 \times 50\ \mu m^2$) from four distinct stages of the cell wall formation (P, P + S_1, P + S_1 + S_2, P + S_1 + S_2 + S_3) as illustrated in Figure 1.

Cellulose I_α shows characteristic IR bands at 3240 and at 750 cm^{-1}, while those for the I_β phase appear at 3270 and at 710 cm^{-1}.[4] In Figure 2, FT-IR spectra in the 1000−650 cm^{-1} region obtained from both wood samples are shown. The IR absorption band at 750 cm^{-1} attributed to the I_α cellulose form appeared only in the spectra from the primary wall (P). This band became weaker with the subsequent deposition of the thick secondary wall layers on the preformed wall layers (P + S_1, P + S_1 + S_2, P + S_1 + S_2 + S_3). On the other hand, the band at 710 cm^{-1} assigned to I_β cellulose was not detected in the spectra for the primary wall, whereas after the start of the secondary wall deposition, it began to appear as a significant shoulder peak. A schematic representation of the developing wood cell wall regions and their corresponding FT-IR spectra are shown in

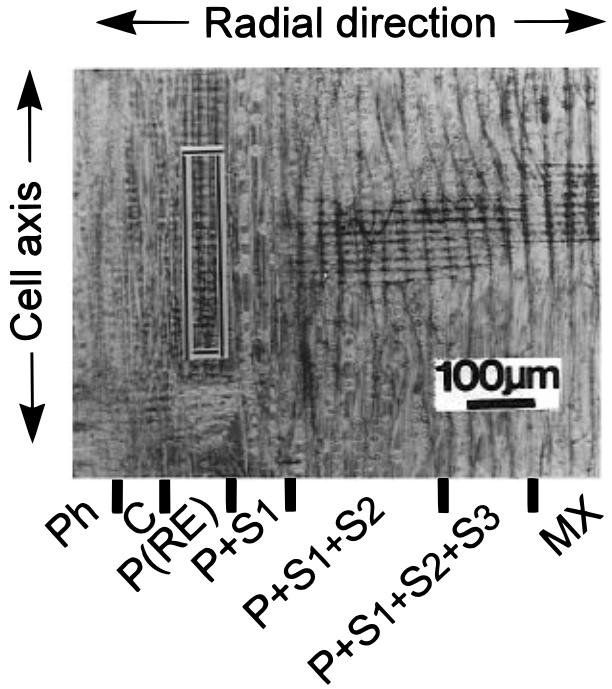

Figure 1. A radial section of Japanese cedar showing differentiating xylem and phloem (Ph). A radial row of developing axial tracheids from the cambial zone (C) to mature xylem (MX) is displayed. The primary wall (P) was formed during radial enlarging (RE) growth. After the enlargement, the outer (S_1), middle (S_2), and inner (S_3) layers of the secondary wall were successively deposited onto the inner surface of the preformed wall. The region outlined in black shows the area analyzed using the microscopic FT-IR attachment.

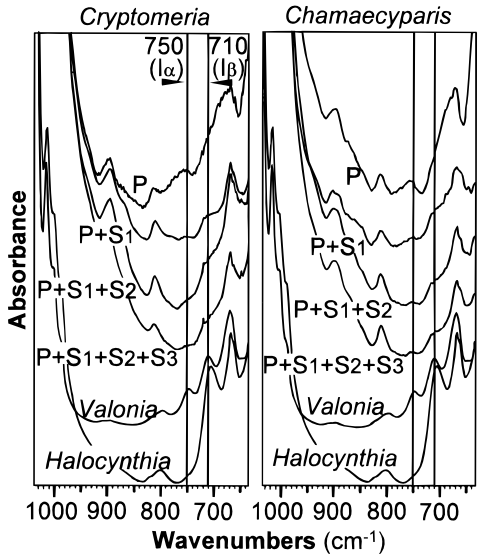

Figure 2. FT-IR spectra of cellulose in the region from 1000 to 650 cm^{-1} from developing Japanese cedar (left) and Japanese cypress (right) tracheid walls composed of P, P + S1, P + S_1 + S_2, and P + S_1 + S_2 + S_3 (abbreviations as noted in Figure 1), compared with standard spectra of cellulose rich in I_α (*Valonia ventricosa*) and pure I_β (*Halocynthia roretzi*) allomorphs. IR absorption bands at 750 and at 710 cm^{-1} are characteristic for the I_α and I_β forms of cellulose, respectively.

* To whom correspondence should be addressed.

S0024-9297(96)00206-9 CCC: $12.00

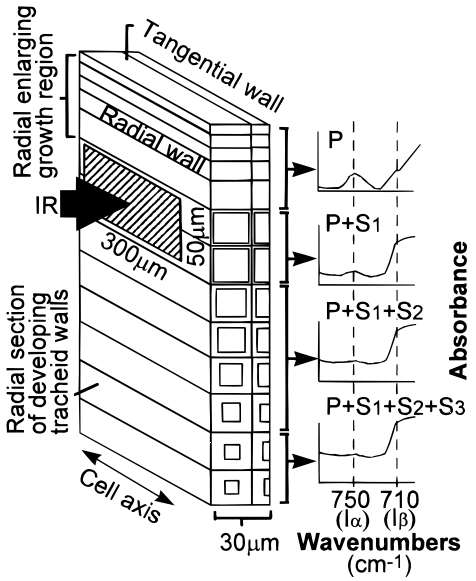

Figure 3. Schematic representation of the cellulose from the four stages in the development of the tracheid walls together with a series of typical FT-IR spectra in the region from 800 to 700 cm^{-1} showing the change in crystalline form from I_α-rich cellulose to I_β-rich cellulose during tracheid wall formation.

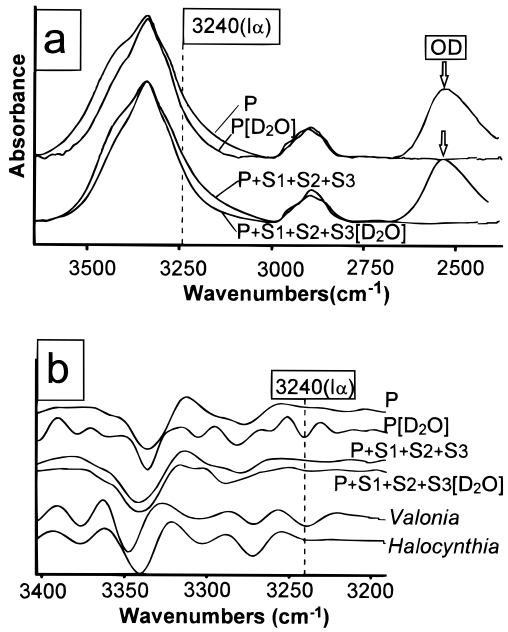

Figure 4. Changes in FT-IR spectra for deuterated cellulose in the region from 3600 to 2400 cm^{-1} (a) and their second derivatives (b) from Japanese cypress tracheid walls composed of P and P + S_1 + S_2 + S_3, compared with standard second-derivative spectra of nondeuterated cellulose rich in I_α (*Valonia ventricosa*) and pure I_β (*Halocynthia roretzi*) allomorphs. The IR absorption band at 3240 cm^{-1} is characteristic for the I_α form of cellulose.

Figure 3. These results show that the cellulose in the primary wall is rich in the Iα phase, whereas the cellulose in the secondary wall is rich in the I_β phase. The IR absorption due to I_α in the primary wall was also detected in the OH stretching region when samples were deuterated. As shown in Figure 4, before deuteration of the sample IR absorptions in this OH stretching region were not clearly evident because of the low crystallinity of wood cellulose and interfering contributions from a variety of OH stretching modes[11] in its amorphous region. After these contributions were reduced by deuteration, however, the absorption due to I_α at 3240 cm^{-1} appeared in the second-derivative spectra for the primary wall, whereas it was not found for the mature wall (P + S1 + S2 + S3).

There are two contradictory reports that wood cellulose is rich in the I_α phase[12] while at the same time the I_β phase is dominant in it.[9] Our IR results can explain this apparent contradiction because the mixture of I_α-rich primary and I_β-rich secondary walls was analyzed concurrently in the samples. Moreover, it has been reported that the electron diffraction patterns of cellulose IV crystal structure were obtained from the primary wall of some higher plant species.[8] However, an IR spectrum we obtained for cellulose IV[13] showed a totally different band pattern from the ones described above. In particular, the band at 750 cm^{-1} did not appear in the spectrum of cellulose IV. In addition, primary wall cellulose has been described as being disorganized cellulose I[8] or totally amorphous.[14] However, we have obtained a result that crystallinity of the tracheid primary wall cellulose can be higher than that of the secondary wall.[15]

Our results also show that the major cellulose crystalline component changes from the metastable triclinic I_α to the stable monoclinic I_β during tracheid wall formation, indicating that there is a different driving force for the crystallization. It may be some interaction among cellulose and these effects, such as the drawing forces exerted by the cellular enlarging growth, the arrangement of the TCs (cellulose-synthesizing terminal enzyme complexes),[4,16] and the affinity of other polysaccharides for cellulose.[5,17] Among these, the drawing force can directly cause aggregation and reorientation of molecules. In fact, during the primary wall formation, tracheid cells extend mainly in their radial diameter to more than twice their initial size.[18] Since the primary wall cellulose crystallizes between the extending plasma membrane (PM) and the drawn cell wall, stresses and strains accordingly produced between two phases can easily accumulate into its nascent cellulose. Moreover, because both ends of nascent molecules are bound, respectively, to the TCs on the PM and to a crystallized cellulose microfibril on the wall, strong stresses should occur along the molecular chains. This whole system is very much like the polymeric crystallization achieved by the drawing of gels. Such a metastable triclinic crystalline phase has also been found in drawn polyethylene gels.[19]

In summary, right after the biosynthesis, mesomorphic state cellulose may be stressed by the cellular enlarging growth to yield the strain-induced I_α phase for the primary wall. After the enlargement ceases, the secondary wall cellulose can be crystallized in a relatively relaxed state which favors the strain-free I_β phase.

Acknowledgment. We thank Dr. A. Isogai for preparing cellulose IV; Mr. E. Tsushima, Mr. R. Nakata, and Dr. K. Takabe for providing native cellulose samples; and Dr. R. S. Werbowyj for a critical reading of the text.

References and Notes

(1) Atalla, R. H.; VanderHart, D. L. *Science* **1984**, *223*, 283−285.
(2) Horii, F.; Yamamoto, H.; Kitamaru, R.; Tanahashi, M.; Higuchi, T. *Macromolecules* **1987**, *20*, 2946−2949.
(3) Sugiyama, J.; Okano, T.; Yamamoto, H.; Horii, F. *Macromolecules* **1990**, *23*, 3196−3198.
(4) Sugiyama, J.; Persson, J.; Chanzy, H. *Macromolecules* **1991**, *24*, 2461−2466.

(5) Yamamoto, H.; Horii, F. *Cellulose* **1994**, *1*, 57−66.
(6) Kataoka, Y.; Saiki, H.; Fujita, M. *Mokuzai Gakkaishi* **1992**, *38*, 327−335.
(7) IR absorptions at 1700−1500 cm^{-1} due to the other contaminants in the samples were decreased to a lesser extent than those for cellulose microcrystals from *Valonia* and *Halocynthia* which were both purified by treatment with a strong acid solution, indicating that the cellulose sample was completely purified.
(8) Chanzy, H.; Imada, K.; Vuong, R.; Barnoud, F. *Protoplasma* **1979**, *100*, 303−316. They confirmed that glucose occupied 96% of total neutral sugars mainly as (1−4)-glucan in the cultured rose cell wall after purification.
(9) Wada, M.; Sugiyama, J.; Okano, T. *Mokuzai Gakkaishi* **1994**, 40, 50−56.
(10) The spectra were the average of 64 scans recorded at a resolution of 4 cm^{-1} with a MCT detector. It was confirmed that the thickness or shape of the samples does not affect the intensity ratio between the IR absorptions for the cellulose I_α and I_β.
(11) Liang, C. Y.; Marchessault, R. H. *J. Polym. Sci.* **1959**, *37*, 385−395.
(12) Tanahashi, M.; Goto, T.; Horii, F.; Hirai, A.; Higuchi, T. *Mokuzai Gakkaishi* **1989**, *35*, 654−662.
(13) Isogai, A.; Usuda, M.; Kato, T.; Uryu, T.; Atalla, R. H. *Macromolecules* **1989**, *22*, 3168−3172.
(14) Nowak-Ossorio, M.; Gruber, E.; Schurz, J. *Protoplasma* **1976**, *88*, 255.
(15) Kataoka, Y.; Kondo, T., unpublished data.
(16) Attala, R. H.; VanderHart, D. L. In *Cellulose and Wood−Chemistry and Technology*; Schuerch, C., Ed.; Wiley-Interscience: New York, 1989; pp 169−188.
(17) For example: Attala, R. H.; Hackney, J. M.; Uhlin, I.; Thompson, N. S. *Int. J. Biol. Macromol.* **1993**, *15*, 109−112.
(18) Wardrop, A. B. In *The Formation of Wood in Forest Trees*; Zimmermann, M. H., Ed.; Academic Press: New York, 1964; pp 87−134.
(19) Chanzy, H.; Smith, P.; Revol, J.-F.; Manley, R. St. J. *Polym. Commun.* **1987**, *28*, 133−136.

MA960206D